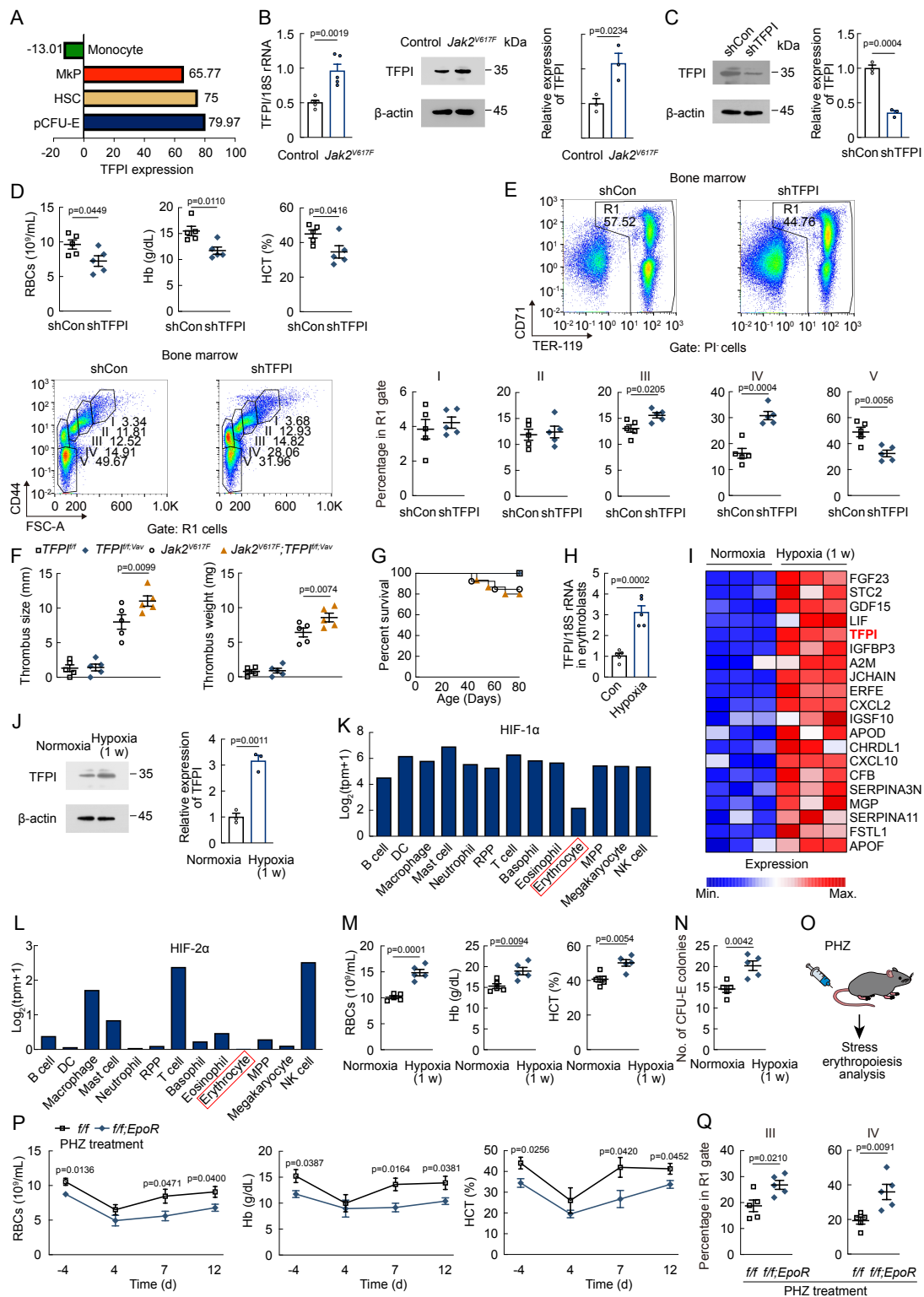# Supplemental Figures



**Figure S1 TFPI affects erythropoiesis in mice.**

(A) Expression of TFPI mRNA in mouse BM cells. Data from Gene Expression

Commons. Numbers next to bars indicate expression level. (B) TFPI expression in

Ter119$^+$ cells of $Jak2^{V617F}$-mutated mice (RT-qPCR, n = 5; Western blot, n = 3). (C) TFPI protein expression of Ter119$^+$ cells after TFPI shRNA treatment (n = 3). (D) PB RBC numbers, Hb, and HCT in shTFPI-treated mice (n = 5). (E) Frequency of erythroblast populations among BM cells in shTFPI-treated mice (n = 5). (F) Thrombus size and weight in $TFPI^{f/f}$ mice, $Jak2^{V617F}$-mutated mice, $TFPI^{f/f;Vav}$ mice, and $Jak2^{V617F};TFPI^{f/f;Vav}$ mice after IVC flow restriction (n = 5). (G) Kaplan-Meier survival analysis of $TFPI^{f/f}$ mice (n = 10), $Jak2^{V617F}$-mutated mice (n = 13), $TFPI^{f/f;Vav}$ mice (n = 10), and $Jak2^{V617F};TFPI^{f/f;Vav}$ mice (n = 15). (H) TFPI mRNA expression in erythroblasts of human EBI after exposed to hypoxia (n = 5). (I) Heatmap showing the top 20 up-regulated secreted protein gene expression in BM cells of hypoxia-exposed mice. (J) TFPI expression in Ter119$^+$ cells of hypoxia-exposed mice (n = 5). (K) HIF-1α mRNA levels of different cell lineages in BM based on Haemosphere (https://www.haemosphere.org). (L) HIF-2α mRNA levels of different cell lineages in BM based on Haemosphere. (M) PB RBC numbers, Hb, and HCT in hypoxia-exposed mice (n = 5). (N) CFU-E number in hypoxia-exposed mice (n = 5). (O) Protocol used for PHZ treatment. (P) PB RBC numbers, Hb and HCT in $TFPI^{f/f;EpoR}$ mice undergoing PHZ-induced stress erythropoiesis (n = 5). (Q) Frequency of RIII and RIV erythroblast populations in $TFPI^{f/f;EpoR}$ mice 6 d after PHZ treatment (n = 5). Statistical analysis was performed using one-way ANOVA (B-F, H, J, M-N, and P-Q). Data are shown as mean ± SEM and are representative of two (D-G and M-Q) or three (B, C, and J) independent experiments. Source data are provided as a Source Data file.
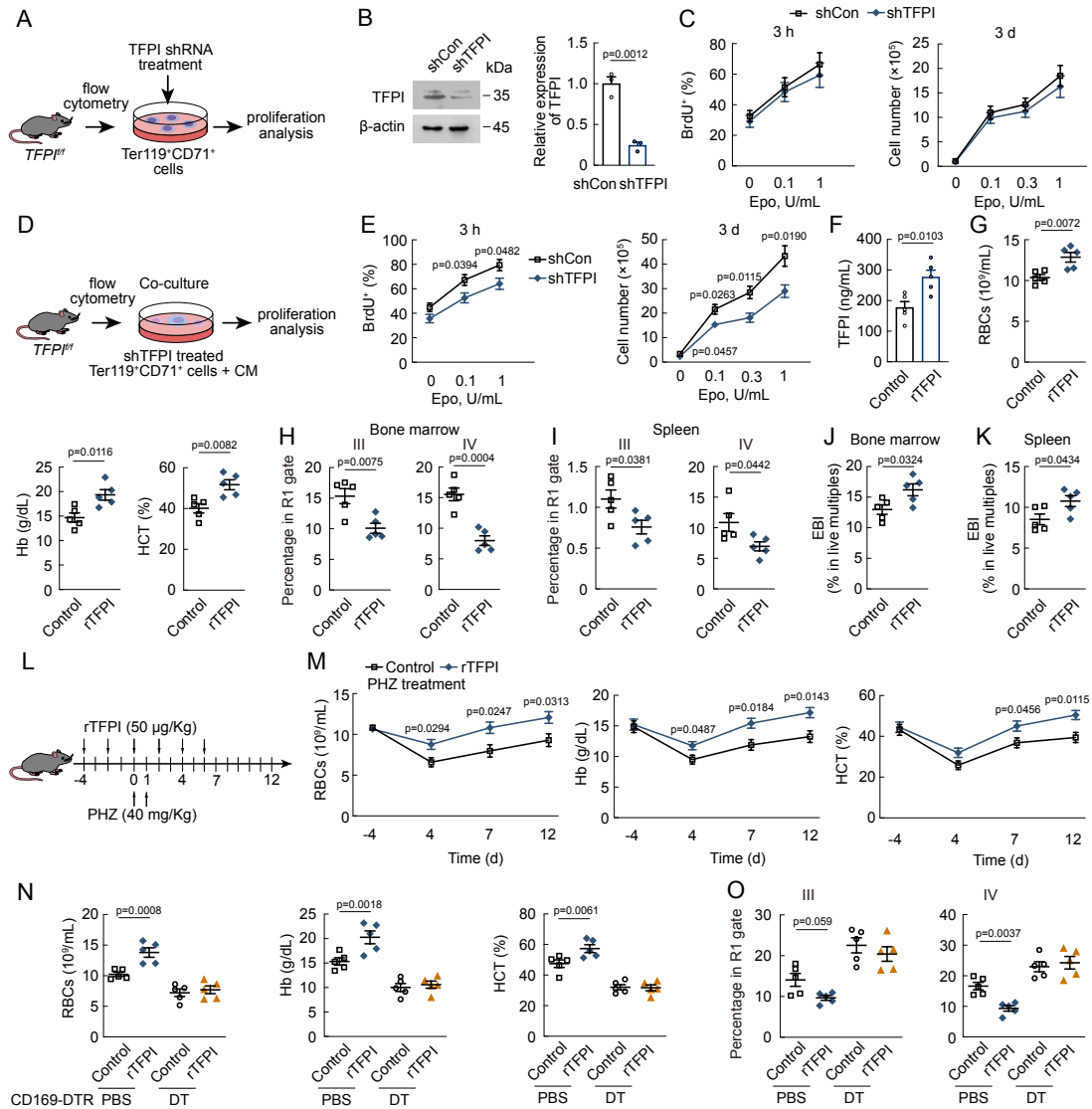
**Figure S2 TFPI treatment improves erythropoiesis.**

(A) Schematic diagram of *in vitro* cultivation and proliferation of Ter119$^+$CD71$^+$ cells.

(B) TFPI protein expression of Ter119$^+$CD71$^+$ cells after TFPI shRNA treatment (n = 3). (C) The expansion of Ter119$^+$CD71$^+$ cells after TFPI shRNA treatment (n = 5). (D) Schematic diagram of proliferation of Ter119$^+$CD71$^+$ cells during co-culture with F4/80$^+$CD169$^+$Vcam-1$^+$ macrophages *in vitro*. (E) The expansion of Ter119$^+$CD71$^+$ cells treated with TFPI shRNA during co-culture with F4/80$^+$CD169$^+$Vcam-1$^+$ macrophages (n = 5). (F) The plasma TFPI concentration of rTFPI-treated mice (n = 5). (G) PB RBC numbers, Hb, and HCT in rTFPI-treated mice (n = 5). (H) Frequency of RIII and RIV erythroblast populations of BM in rTFPI-treated mice (n = 5). (I)

Frequency of RIII and RIV erythroblast populations of spleen in rTFPI-treated mice (n = 5). (J) EBI numbers in the BM of rTFPI-treated mice (n = 5). (K) EBI numbers in the spleen of rTFPI-treated mice (n = 5). (L) Experimental scheme for PHZ-induced stress erythropoiesis. (M) PB RBC numbers, Hb, and HCT in rTFPI-treated mice undergoing PHZ-induced stress erythropoiesis (n = 5). (N) PB RBC numbers, Hb, and HCT in CD169$^{DTR/+}$ mice after DT and rTFPI treatment (n = 5). (O) Frequency of RIII and RIV erythroblast populations of BM in CD169$^{DTR/+}$ mice after DT and rTFPI treatment (n = 5). Statistical analysis was performed using one-way ANOVA (B, E-K, and M-O). Data are shown as mean ± SEM and are representative of two (F-K and M-O) or three (B, C, and E) independent experiments. Source data are provided as a Source Data file.
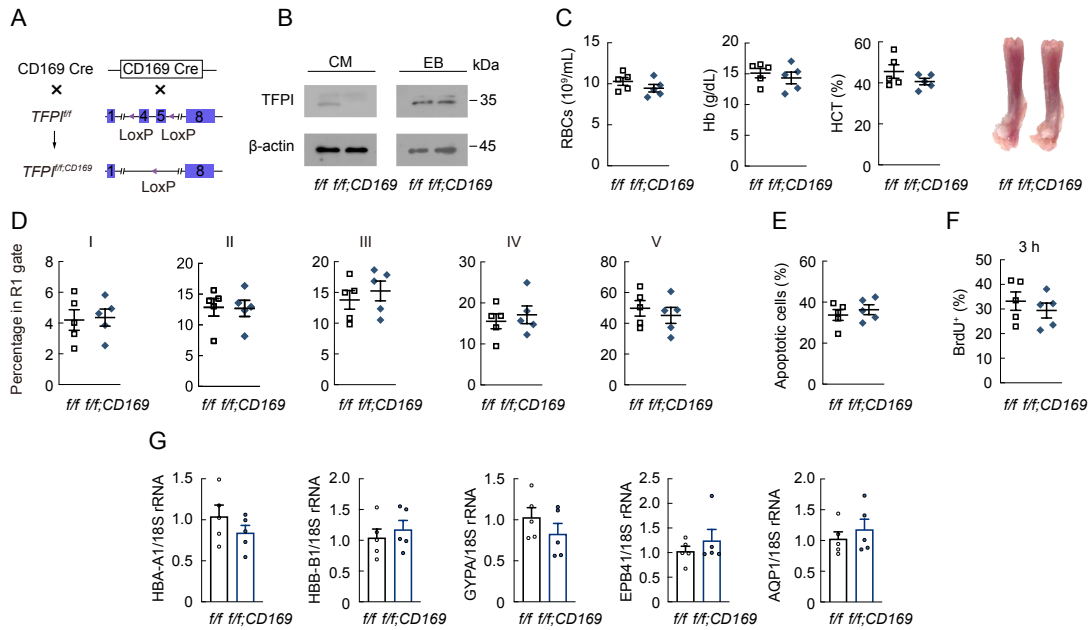
4

**Figure S3 Macrophage-specific TFPI knockout does not affect erythropoiesis in mice.**

(A) Protocol used to prepare *TFPI^{f/f;CD169}* mice. (B) TFPI protein expression in CM and erythroblasts of *TFPI^{f/f;CD169}* mice (n = 3). (C) PB RBC numbers, Hb, and HCT in *TFPI^{f/f;CD169}* mice (n = 5). (D) Frequency of erythroblast populations among BM cells in *TFPI^{f/f;CD169}* mice (n = 5). (E) Frequency of apoptotic erythroblasts among BM cells in *TFPI^{f/f;CD169}* mice (n = 5). (F) BrdU incorporation assay for erythroblasts proliferation of *TFPI^{f/f;CD169}* mice (n = 5). (G) HBA-A1, HBB-B1, GYPA, EPB41 and AQP1 mRNA expression in erythroblasts among BM cells of *TFPI^{f/f;CD169}* mice (n = 5). Data are shown as mean ± SEM and are representative of two (C and D) or three (B, E-G) independent experiments. Source data are provided as a Source Data file.
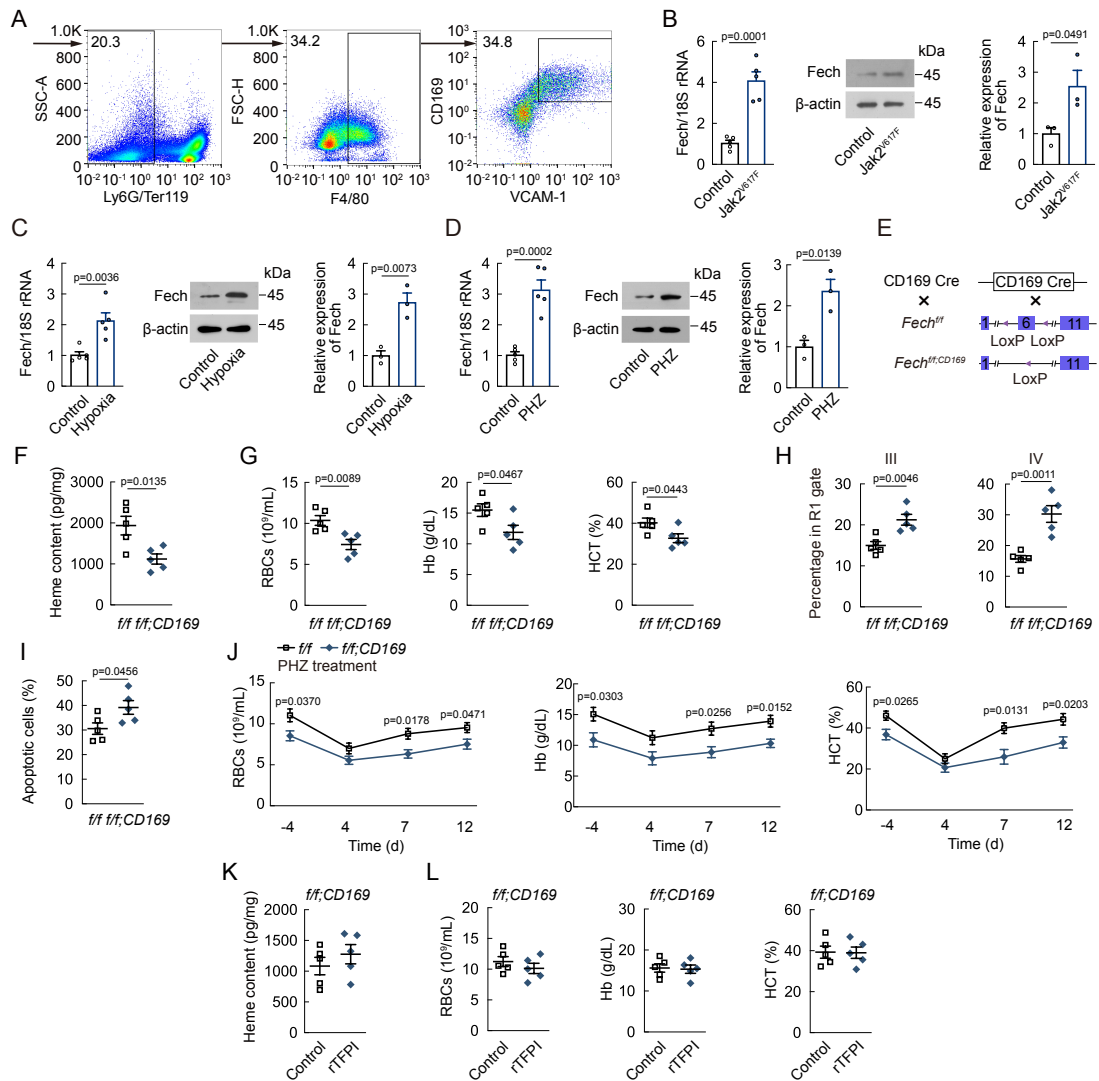
**Figure S4 Heme in F4/80⁺CD169⁺Vcam-1⁺ macrophages improves erythropoiesis**.

(A) Representative FACS plots of the $F4/80^+CD169^+Vcam\text{-}1^+$ macrophage gating strategy. (B) Fech expression in $F4/80^+CD169^+Vcam\text{-}1^+$ macrophages of $Jak2^{V617F}$-mutated mice (RT-qPCR, n = 5; Western blot, n = 3). (C) Fech expression in $F4/80^+CD169^+Vcam\text{-}1^+$ macrophages of hypoxia-exposed mice (RT-qPCR, n = 5; Western blot, n = 3). (D) Fech expression in $F4/80^+CD169^+Vcam\text{-}1^+$ macrophages of PHZ-treated mice (RT-qPCR, n = 5; Western blot, n = 3). (E) Protocol to prepare $Fech^{f/f;CD169}$ mice. (F) Heme content in $F4/80^+CD169^+Vcam\text{-}1^+$ macrophages of $Fech^{f/f;CD169}$ mice (n = 5). (G) PB RBC numbers, Hb, and HCT in $Fech^{f/f;CD169}$ mice (n = 5). (H) Frequency of RIII and RIV erythroblast populations in $Fech^{f/f;CD169}$ mice (n =

5). (I) Frequency of apoptotic erythroblasts among BM cells in *Fech^{f/f;CD169}* mice (n = 5). (J) PB RBC numbers, Hb, and HCT in *Fech^{f/f;CD169}* mice after PHZ treatment (n = 5). (K) Heme content in F4/80$^+$CD169$^+$Vcam-1$^+$ macrophages of *Fech^{f/f;CD169}* mice after rTFPI treatment (n = 5). (L) PB RBC numbers, Hb, and HCT in *Fech^{f/f;CD169}* mice after rTFPI treatment (n = 5). Statistical analysis was performed using one-way ANOVA (B-D, and F-L). Data are shown as mean ± SEM and are representative of two (F-L) or three (B-D) independent experiments. Source data are provided as a Source Data file.
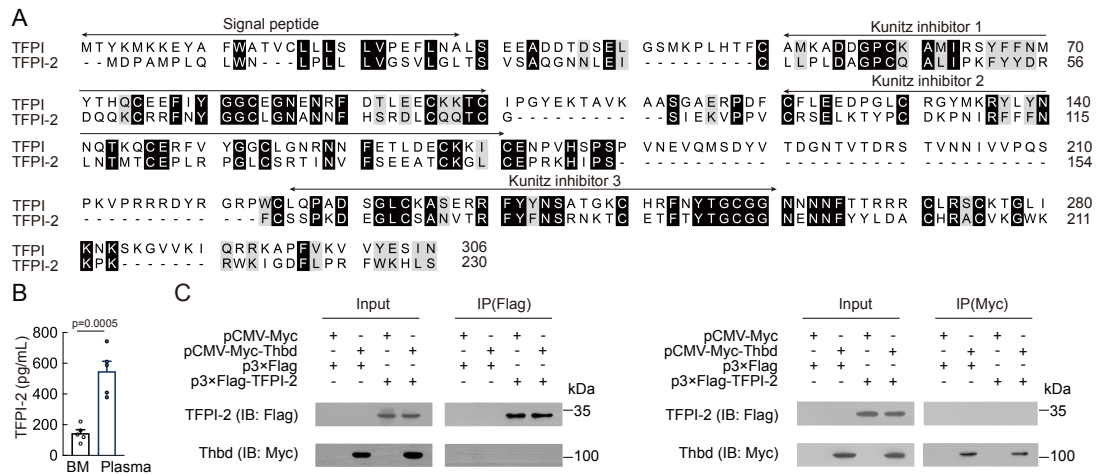
**Figure S5 Thbd does not interact with TFPI-2.**

(A) Multiple alignment of the amino acid sequences of TFPI and TFPI-2 in mice. (B) TFPI-2 protein expression in BM and plasma (n = 5). (C) Co-IP analysis of the interaction between Thbd and TFPI-2 in HEK293T cells (n = 2). Statistical analysis was performed using one-way ANOVA (B). Data are shown as mean ± SEM and are representative of two (C) or three (B) independent experiments. Source data are provided as a Source Data file.
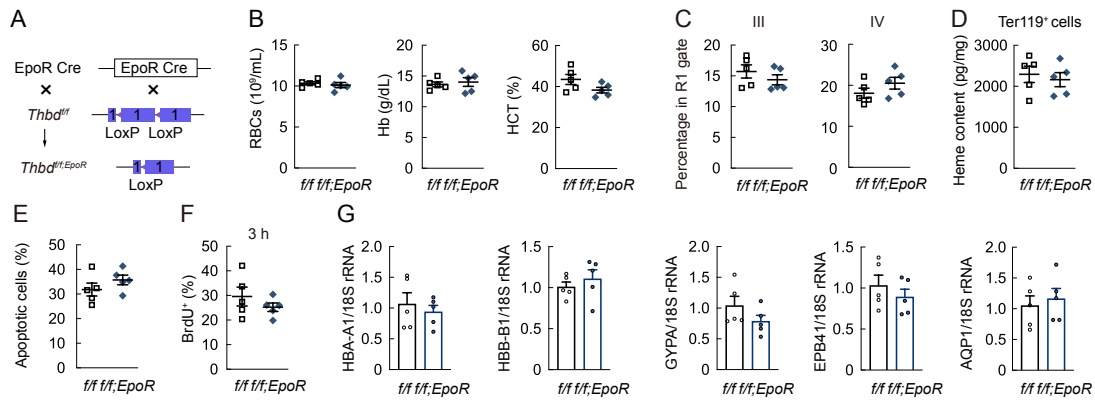
**Figure S6 Erythroid-specific Thbd knockout does not affect erythropoiesis in mice.**

(A) Protocol used to prepare *Thbd*^f/f;EpoR^ mice. (B) PB RBC numbers, Hb, and HCT in *Thbd*^f/f;EpoR^ mice (n = 5). (C) Frequency of erythroblast populations among BM cells in *Thbd*^f/f;EpoR^ mice (n = 5). (D) Heme content in Ter119$^+$ cells of *Thbd*^f/f;EpoR^ mice (n = 5).

(E) Frequency of apoptotic erythroblasts among BM cells in *Thbd*^f/f;EpoR^ mice (n = 5).

(F) BrdU incorporation assay for erythroblasts proliferation of *Thbd*^f/f;EpoR^ mice (n = 5).

(G) HBA-A1, HBB-B1, GYPA, EPB41 and AQP1 mRNA expression in erythroblasts among BM cells of *Thbd*^f/f;EpoR^ mice (n = 5). Data are shown as mean ± SEM and are representative of two (B-D) or three (E-G) independent experiments. Source data are provided as a Source Data file.
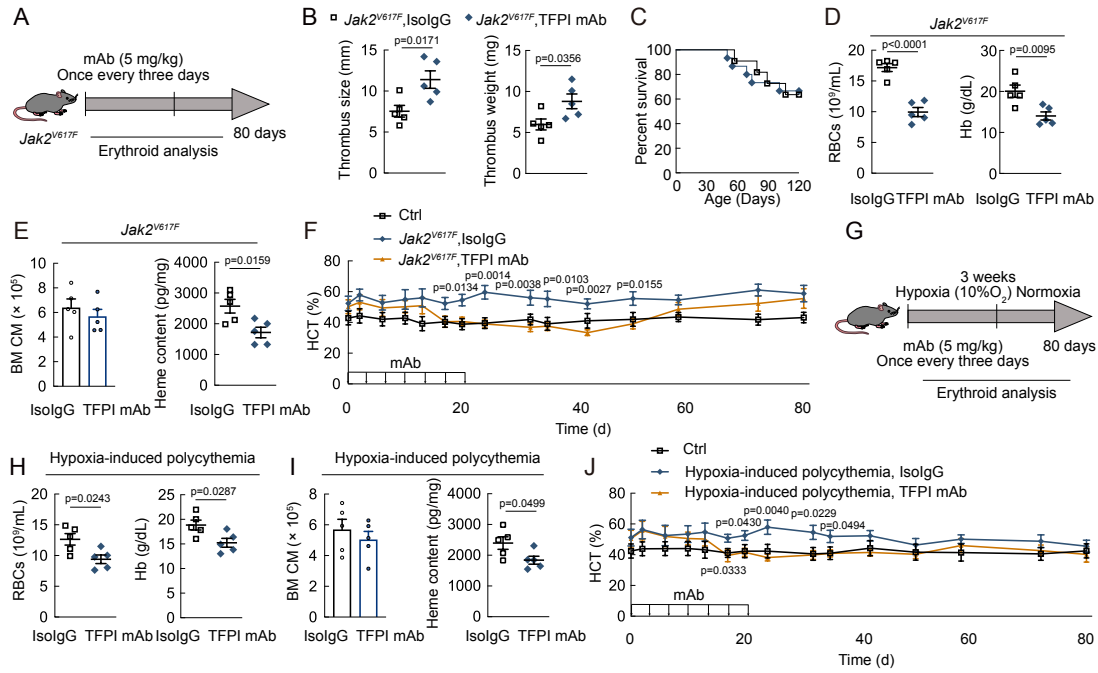
**Figure S7 Effects of anti-TFPI antibody on hypoxia- and *Jak2^V617F*-induced polycythemia.**

(A) Schematic of experimental design for TFPI mAb treatment of *Jak2^V617F*-mutated mice. (B) Thrombus size and weight in *Jak2^V617F*-mutated mice and TFPI mAb-treated *Jak2^V617F*-mutated mice after IVC flow restriction. (C) Kaplan-Meier survival analysis of *Jak2^V617F*-mutated mice (n = 11) and TFPI mAb-treated *Jak2^V617F*-mutated mice (n = 15). (D) PB RBC numbers and Hb in *Jak2^V617F*-mutated mice after TFPI mAb treatment (n = 5). (E) The numbers of F4/80$^+$CD169$^+$Vcam-1$^+$ macrophages per femur and F4/80$^+$CD169$^+$Vcam-1$^+$ macrophage heme content of *Jak2^V617F*-mutated mice after TFPI mAb treatment (n = 5). (F) HCT in control and *Jak2^V617F*-mutated mice after treated with IsoIgG and TFPI mAb (n = 5). (G) Schematic of experimental design for construction of a mouse model of hypoxia-induced polycythemia. (H) PB RBC numbers and Hb in hypoxia-induced polycythemia mice after TFPI mAb treatment for 3 weeks (n = 5). (I) The numbers of F4/80$^+$CD169$^+$Vcam-1$^+$ macrophages per femur and F4/80$^+$CD169$^+$Vcam-1$^+$ macrophage heme content of hypoxia-induced

polycythemia mice after TFPI mAb treatment for 3 weeks (n = 5). (J) HCT in control

and hypoxia-induced polycythemia mice after treated with IsoIgG and TFPI mAb (n =

5). Statistical analysis was performed using one-way ANOVA (B,D-F, and H-J). Data

are shown as mean ± SEM and are representative of two independent experiments.

Source data are provided as a Source Data file.

**Supplemental Tables**

**Supplementary Table 1.** The list of candidate TFPI-interacting proteins identified by yeast-two-hybrid analyses.

| Ensembl | Positive gene identified | positive clones/total identical clones |
|---|---|---|
| ENSMUSG00000031444 | F10 | 3/30 |
| ENSMUSG00000074743 | Thbd | 8/30 |
| ENSMUSG00000055436 | Srsf11 | 15/30 |
| ENSMUSG00000027249 | F2 | 1/30 |
| ENSMUSG00000024097 | Srsf7 | 17/30 |
| ENSMUSG00000022961 | Son | 18/30 |

**Supplementary Table 2.** Characteristics of patient and healthy cohorts.

| | healthy cohorts | patient cohorts |
|---|---|---|
| Number of patient/healthy cohort | 18 | 21 |
| Male | 7 | 10 |
| Female | 11 | 11 |
| Median age for samples (years) | 40 | 37 |

**Supplementary Table 3.** Primers used for RT-qPCR.

| **RT-qPCR** | |
|---|---|
| Genes | Primers |
| Mouse | |
| TFPI | Forword 5'CCTTCCCCAGTGAATGAGGT3' |
| | Reverse 5'ATCCACTGTCTGCTGGTTGA3' |
| Fech | Forword 5'TGACCACATTGAGACGCTCT3' |
| | Reverse 5'GCTTGTTGGACTGGATGTGG3' |
| Thbd | Forword 5'GGCTGGAGATGACCCAGATA3' |
| | Reverse 5'GAAACAACGGTAAGGGCAAA3' |
| CD71 | Forword 5'AGCCAGATCAGCATTCTCTAACT3' |
| | Reverse 5'GCCTTCATGTTATTGTCGGCAT3' |
| ALAS2 | Forword 5'CACCTATGCTTAAGGAGCCA3' |

|  |  |
|------|------|
|  | Reverse 5'CAGAAGCACACAGGAAAGCA3' |
| ALAD | Forword 5'GTTCTGCACAGCGGCTACTT3' |
|  | Reverse 5'AGCTGGTTTACGCCATACCTG3' |
| HMBS | Forword 5'AAGGGCTTTTCTGAGGCACC3' |
|  | Reverse 5'AGTTGCCCATCTTTCATCACTG3' |
| UROS | Forword 5'GCAGTGAAGCTGTGTTTGGA3' |
|  | Reverse 5'GCAAGCTTTTCTGCATTTCC3' |
| UROD | Forword 5'CCTCTGGATGCTGCCATAAT3' |
|  | Reverse 5'TAAGGGTGATGGCTTGGAAC3' |
| CPOX | Forword 5'ATGCCCTTCTTGGGAACTTT3' |
|  | Reverse 5'TAGCCCTGGCTGGACTAGAA3' |
| PC | Forword 5'GGTGCTCATCCACACTTCCT3' |
|  | Reverse 5'GCAGATGGGCACTATGGTTT3' |
| TF | Forword 5'TGCTTCTCGACCACAGACAC3' |
|  | Reverse 5'TAAAAACTTTGGGGCGTTTG3' |
| Human |  |
| TFPI | Forword 5'ATGGAACCCAGCTCAATGCT3' |
|  | Reverse 5'GGCACGACACAATCCTCTGT3' |
| Thbd | Forword 5'ACATCCTGGACGACGGTTTC3' |
|  | Reverse 5'CGCAGATGCACTCGAAGGTA3' |
| TF | Forword 5'AGACAGCCCGGTAGAGTGTA3' |
|  | Reverse 5'AGCCAGGATGATGACAAGGAT3' |
| Fech | Forword 5'TTGTTCTCTAAGGCCCTGGC3' |
|  | Reverse 5'GCGGACAGCTCAGGGTCA3' |

**Supplementary Table 4.** Target sequences for shRNA.

| shRNA |  |
|------|------|
| Lentivirus | Sequences |
| Mouse TFPI shRNA | 5'CCATGCAAAGCAATGATAAGGAGTT3' |
| Human TFPI shRNA | 5'ACAGTGTGAACGTTTCAAGTA3' |
| Mouse GATA1 shRNA | 5'GAGGAAATGGAGGAGGCCTTGAAGA3' |
| Mouse Thbd shRNA | 5'GCCCACATCTCTAGTACCTACAACA3' |
| Mouse aPC shRNA | 5'CATGCGCTGCAAGTCCACTGTGAAT3' |